Experimental Animals
Exp. Anim. 72(3), 302–313, 2023

Original

SRY-box transcription factor 9 modulates Müller cell gliosis in diabetic retinopathy by upregulating TXNIP transcription

Sheng LI, Gaoxiang OUYANG, Linhui YUAN, Xiaoxuan WU and Lijun ZHANG

Department of Ophthalmology, Dalian No. 3 People's Hospital, No. 40, Qianshan Road, Ganjingzi District, Dalian, Liaoning, 116033, P.R. China

Abstract: Diabetic retinopathy (DR), a common complication of diabetes, involves excessive proliferation and inflammation of Muller cells and ultimately leads to vision loss and blindness. SRY-box transcription factor 9 (SOX9) has been reported to be highly expressed in Müller cells in light-induced retinal damage rats, but the functional role of SOX9 in DR remains unclear. To explore this issue, the DR rat model was successfully constructed via injection with streptozotocin (65 mg/kg) and the retinal thicknesses and blood glucose levels were evaluated. Müller cells were treated with 25 mmol/l glucose to create a cell model in vitro. The results indicated that SOX9 expression was significantly increased in DR rat retinas and in Müller cells stimulated with a high glucose (HG) concentration. HG treatment promoted the proliferation and migration capabilities of Müller cells, whereas SOX9 knockdown reversed those behaviors. Moreover, SOX9 knockdown provided protection against an HG-induced inflammatory response, as evidenced by reduced tumor necrosis factor-α, IL-1β, and IL-6 levels in serum and decreased NLRP3 inflammasome activation. Notably, SOX9 acted as a transcription factor that positively regulated thioredoxin-interacting protein (TXNIP), a positive regulator of Müller cells gliosis under HG conditions. A dual-luciferase assay demonstrated that SOX9 could enhance TXNIP expression at the transcriptional level through binding to the promoter of *TXNIP*. Moreover, TXNIP overexpression restored the effects caused by SOX9 silencing. In conclusion, these findings demonstrate that SOX9 may accelerate the progression of DR by promoting glial cell proliferation, metastasis, and inflammation, which involves the transcriptional regulation of TXNIP, providing new theoretical fundamentals for DR therapy.

Key words: diabetic retinopathy, inflammation, Müller cell gliosis, SRY-box transcription factor 9 (SOX9), *TXNIP* promoter

Introduction

Diabetic retinopathy (DR), a microvascular complication of type 1 and type 2 diabetes, is characterized by exudation edema, hemorrhage, neovascularization, and the formation of a proliferation membrane on the retina, causing optic nerve impairment [1]. Increasing evidence indicates that DR is one of the most serious blinding diseases in the world [2, 3]. Statistically, the ratio of blindness caused by DR ranges from 15–17% in developed areas [4]. Notably, it is reported that oxidative stress, apoptosis, and inflammation can promote the development of DR [5, 6]. Studies in diabetic mice demonstrated that inflammatory processes aggravated the occurrence of DR by upregulating the expression of a pro-inflammatory cytokine [7].

SRY-box transcription factor 9 (SOX9), a member of the SOX transcription factor family, maps to chromosome 17 characterized by the high mobility group of boxes, mediating cell survival by activating genes that

(Received 16 September 2022 / Accepted 5 January 2023 / Published online in J-STAGE 16 January 2023)
Corresponding author: L. Zhang. email: drzhanglijun@126.com

maintain pluripotency [8]. Increasing evidence indicates that high glucose (HG) concentration could upregulate the expression level of SOX9 in Müller cells [9]. In addition, Wang *et al.* showed that knockdown of SOX9 decreased glial fibrillary acidic protein (GFAP) expression, indicating that SOX9 could induce reactive gliosis in Müller cells of rats [10]. SOX9 expression was associated with cell proliferation and migration. In mouse models of pulmonary fibrosis, the migration of pulmonary fibroblasts was inhibited following SOX9 knockdown [11]. Notably, the inflammatory reaction was also regulated by SOX9 expression. In chondrocytes cultured in vitro, the upregulation of SOX9 aggravated the inflammation process by activating the nuclear transcription factor-κB signaling pathway, and SOX9 knockdown inhibited chondrocyte proliferation [12]. However, the regulatory role and specific mechanism involved in the effect of SOX9 on DR are still unknown.

Thioredoxin-interacting protein (TXNIP), a positive regulator of Müller cells gliosis, is highly expressed in various tissues under HG treatment [13, 14]. TXNIP has been found to regulate various biological reactions, such as the proliferation of glial cells, and the occurrence of apoptosis, autophagy, and inflammation responses [15, 16]. In the middle and final stages of peripheral nerve injury, TXNIP knockdown was found to inhibit Schwann cell migration caused by the receptor for advanced glycation end products [17]. Furthermore, overexpression of TXNIP promoted the migration of human aortic smooth muscle cells in a model of atherosclerosis [18]. Further mechanistic studies reported that the downregulation of TXNIP exerted protective effects against DR damage by inhibiting the expression of GFAP and gliosis in Müller cells [19, 20]. The *TXNIP* promoter is sensitive to HG. Recent research by Lalit *et al.* suggested that HG could promote the activities of the *TXNIP* promoters, further enhancing the transcriptional expression of TXNIP [21]. However, how HG regulates the activities and the transcriptional expression of the *TXNIP* promoters is entirely unclear.

In the present study, we aimed to investigate the regulatory role of SOX9 in cell function in the progression of streptozotocin (STZ)-induced DR, an acknowledged model of type 1 DR. The expression of SOX9 and TXNIP in DR retinal tissues and HG-treated Müller cells was examined. In addition, the functional effects of SOX9 on cell viability, migration, and inflammatory responses were examined in HG-induced Müller cells. Furthermore, the association between SOX9 and TXNIP was explored by dual-luciferase analysis, and the results demonstrated that SOX9 transcriptionally regulated TXNIP expression. The function of SOX9 knockdown was reversed following TXNIP overexpression. Collectively, these findings indicated that SOX9 played important roles in hyperglycemia-induced DR and that SOX9 exerted functions through the regulation of TXNIP.

Materials and Methods

Animal model

In the animal experiments, all the procedures were strictly conducted in consideration of the welfare of all animals and were in accordance with the Guide for Care of Dalian No. 3 People's Hospital and approved by the Ethics Committee of the same institution (No. 2020-KT-006). Healthy adult male Sprague Dawley rats were maintained under a 12 h light/dark cycle at a temperature of 21–23°C and 45–55% humidity for one week. Streptozotocin (STZ) has been shown to destroy pancreatic island β cells and commonly used for the induction of DR in animals [22]. Rats were randomly groups: the STZ and control groups. The rats in the STZ group were intraperitoneally (i.p.) injected with STZ (65 mg/kg, Aladdin, Shanghai, China) dissolved in sodium citrate buffer, and the rats in the control group received the same volume of sodium citrate buffer. At 3 days after injection, the rats in the STZ group were considered diabetic rats based on their blood glucose concentrations (>20 mmol/l) and applied in the following experiments. All rats were sacrificed at the end of four weeks, and bilateral eyes were enucleated and fixed in 4% paraformaldehyde at 4°C overnight. The whole retinas were then dissociated, and sections were cut in the same orientation and always through the optic nerve head for subsequent histopathological analysis.

Hematoxylin and eosin (H&E) staining

Enucleated eyeballs were fixed in 4% paraformaldehyde and embedded in paraffin. Retinal tissues were sectioned in the same orientation at a thickness of 5 μm. The paraffin-embedded sections were deparaffinized and subjected to H&E staining for conventional histopathologic examination of DR. Images were captured under a light microscope (200×; Olympus, Tokyo, Japan). The total retina was defined as the distance between the ganglion cell layer (GCL) and the photoreceptor layer [23]. The thickness of the total retina was evaluated using the Image-Pro Plus 6.0 analysis software.

Cell culture and treatment

Müller cells were obtained from Chi Scientific (Nanjing, China) and maintained in Dulbecco's modified Eagle's medium (DMEM)/F12 medium (Gibco, Thermo

Fisher Scientific, Waltham, MA, USA) containing 10% fetal bovine serum at 37°C with 5% CO_2. Cells were cultured in a medium with 5.5 mmol/l glucose (NG group, MCE, Monmouth Junction, NJ, USA) and 25 mmol/l glucose (HG group), respectively. Müller cells were cultured and infected with lentivirus. A lentivirus carrying short hairpin RNA (shRNA) against SOX9 (sh-SOX9) was constructed to knock down SOX9, and a lentivirus containing negative control shRNA (shNC) was constructed as a control. For TXNIP overexpression, the *Rattus* TXNIP coding sequence was inserted into the lentiviral plasmids. Meanwhile, cells infected with an empty recombinant lentivirus were used as controls. After transfection for 72 h, the cells were co-incubated with 25 mmol/l glucose at 37°C with 5% CO_2. Finally, the cells and supernatant were collected for further experiments.

Analysis of cell viability

The methyl thiazole tetrazolium (MTT) assay was conducted to detect cell viability. In brief, following transfection and treatment, around 6×10^3 Müller cells were cultured in 96-well plates for 0, 24, 48, 72, and 96 h, respectively. Subsequently, 0.5 mg/ml of MTT reagent (Beyotime, Shanghai, China) was added to each well and cultured at 37°C with 5% CO_2 for another 4.5 h. Following cultivation, dimethyl sulfoxide (150 μl) was added, and the cells were cultivated for 10 min in the dark. Cell viability was determined using a microplate reader (Agilent Technologies, Winooski, VT, USA) at 570 nm.

Determination of inflammatory cytokines contents

The concentrations of tumor necrosis factor-α (TNF-α), IL-1β, and IL-6 in the supernatant fluid of Müller cells were determined using ELISA kits (MultiSciences Biotech, Hangzhou, China) following the manufacturer's protocol. The absorbance at 450 nm was measured using a microplate reader (Agilent Technologies).

Dual-luciferase reporter assay

For detection of the correlation between SOX9 and TXNIP predicted by the JASPAR website, Müller cells were co-transfected with the *TXNIP* promoter-reporter vectors and SOX9 overexpression vectors. After transfection for 48 h, the cells were washed twice with PBS (Sangon, Shanghai, China), and 250 μl of cell lysis buffer (KeyGen Biotech, Nanjing, China) was then added. The luciferase activity was determined using the Dual-Luciferase Reporter Assay Kit (KeyGen BioTech) following the manufacturer's protocol. *Renilla* luciferase activity was used as an internal control.

Wound healing assay

Wound healing assays were conducted to assess Müller cell migration. After transfection and treatment, cells were treated with 1 μg/ml of mitomycin C (Sigma-Aldrich, MilliporeSigma, St. Louis, MO, USA) in the serum-free medium for 1 h. Subsequently, the cells in each group were scratched using 200 μl pipette tips and washed with a serum-free medium to remove cell debris. The wound gap area was visualized with a microscope (100×; Olympus) at 0, 12, and 24 h. The migration distances of the experimental groups were calculated.

Immunofluorescence staining

For immunofluorescence staining, the paraffin-embedded sections were dewaxed and dehydrated with gradient alcohol. Following antigen repaired in the original repair solution, the sections were blocked with 1% bovine serum albumin (BSA; Sangon) for 15 min and incubated with primary antibodies against SOX9 (1:100; ABclonal, Wuhan, China) and GFAP (1:100; ABclonal) at 4°C overnight. Then, retinas were nurtured with a secondary antibody (1:200; Invitrogen, Carlsbad, CA, USA) for 60 min, followed by counterstaining with DAPI (Aladdin).

For the cell immunofluorescence experiments, the cell climbing sheets were fixed in 4% paraformaldehyde. After permeabilization in 0.1% Triton X-100 (Beyotime), the slides were blocked with 1% BSA. The slides were then incubated with SOX9 antibody (1:200, ABclonal) overnight, bound antibodies were detected with Cy3-labeled secondary antibody rabbit IgG (1:200, Invitrogen) for 1 h, and the slides were incubated with DAPI. All stained sections and the cell climbing slides were visualized with a fluorescence microscope (400×; Olympus).

Real-time PCR analysis

Total RNA was obtained from retinal tissue samples and cells treated with TRIpure (Bioteke, Beijing, China). Subsequently, first-strand cDNA for real-time PCR was generated using Super M-MLV Reverse Transcriptase (Bioteke). The real-time PCR reaction system was constructed according to the instructions of a SYBR Green kit (Solarbio, Beijing, China). Data were calculated by the $2^{-\Delta\Delta CT}$ method and standardized to the housekeeping gene *GAPDH*. The real-time PCR primers were used as follows: for *SOX9* 5′-GCACATCAAGACGGAGCAA-3′ (F) and 5′-AGGTGAAGGTGGAGTAGAGCC-3′ (R); for *TXNIP* 5′-ACGCTGACTTTGAGAACAC-3′ (F) and 5′-AGCCAGGGACACTAACATA-3′ (R).

Western blot analysis

Total proteins were isolated from retinal tissues and

cells with RIPA buffer containing PMSF protease inhibitor (Solarbio). The concentration of proteins was measured with a BCA assay kit (Solarbio). Western blot protocol was performed according to standard procedures. The antibodies included SOX9 (1:1,000, ABclonal), TXNIP (1:1,000; ABclonal), NLRP3 (1:1,000; ABclonal), cleaved caspase-1 (1:500; Affinity, Cincinnati, OH, USA), and rabbit IgG (1:3,000, Solarbio). Visualization of the bands was performed using an enhanced chemiluminescence kit (Solarbio).

Statistical analysis

All data were statistically analyzed with Tukey's unpaired *t*-test or multiple comparison one-way analysis of variance (ANOVA) using the GraphPad Prism software 9. Results were expressed as the mean ± SD. A *P*-value <0.05 was considered to indicate a statistically significant difference.

Results

Effects of STZ-induced diabetes on the expression of SOX9 and TXNIP in the rat retina

An STZ induced-diabetes model was successfully established, and the blood glucose levels in the control and STZ groups were determined. As indicated in Fig. 1A, the blood glucose levels in the STZ group were significantly increased, confirming that the STZ-induced DR model was successfully established. The expression of SOX9 and TXNIP in the retina was detected by Western blot and real-time PCR assay. Markedly increased mRNA and protein expression levels of SOX9 and TXNIP were observed in the STZ group, as shown in Fig. 1B. In addition, retinal thickness was measured using H&E staining after tissue harvest, and the total thickness was defined and quantified in the control and STZ groups. The results revealed that the thickness of all retinal layers was significantly reduced in the STZ group compared with the control group (Fig. 1C). Immunofluorescence staining was performed to detect the expression and location of SOX9 and GFAP in retinas. As indicated in Fig. 1D, SOX9 immunoreactivity was mainly localized to the outer nuclear layer (ONL) in the control group. It was substantially increased in the diabetic retina, and it was augmented and variably extended into the inner nuclear layer (INL) and ganglion cell layer (GCL). Concurrently, Müller glial cells, labeled by GFAP, were restricted to the retinal GCL in the control group (Fig. 1E). However, GFAP immunoreactivity was augmented and variably extended into the outer plexiform layer (OPL) and ONL in the diabetic retina. These results revealed that SOX9 and TXNIP were significantly expressed in the retinas of rats with STZ-induced diabetes and that retinal injury may lead to gliosis.

Effects of SOX9 on HG-induced proliferation and migration in Müller cells

The effect of SOX9 on cell proliferation and migration was determined in HG-induced Müller cells. As shown in Fig. 2A, HG induced a significant increase in the mRNA and protein expression levels of SOX9. Meanwhile, immunofluorescence analyses revealed that the expression levels of SOX9 were elevated in the cells following HG treatment (Fig. 2B), which was consistent with *in vivo* experiments. To further explore the regulatory role of SOX9, the expression of SOX9 was silenced under HG conditions, and the transfection efficiency was confirmed by Western blot assay (Fig. 2C). Subsequently, we identified the effect of SOX9 on HG-induced proliferation of Müller cells *in vitro*. As demonstrated in Fig. 2D, HG caused a time-dependent trend of increased cell viability. Conversely, cell viability was decreased by SOX9 knockdown in Müller cells treated with HG. In addition, the specific effect of SOX9 on HG-induced migration of Müller cells was further explored. As shown in Figs. 2E and F, the results of the wound healing assay showed that HG treatment significantly increased the migratory abilities of Müller cells, while SOX9 knockdown significantly suppressed the elevated mobility under HG conditions.

Effects of SOX9 on the HG-induced inflammation response in Müller cells

To further investigate the effect of SOX9 expression on the inflammation reaction induced by HG, we first detected the levels of the inflammatory cytokines TNF-α and IL-6 by ELISA assay in the cells treated with HG for 48 h. As shown in Fig. 3A, HG treatment increased the secretion of TNF-α and IL-6, while SOX9 silencing suppressed the increased expression of the inflammatory cytokines after HG stimulation. In addition, activation of the NLRP3 inflammasome was evaluated in HG-induced Müller cells, as evidenced by the increased protein levels of NLRP3 and cleaved caspase-1, whereas SOX9 knockdown attenuated NLRP3 inflammasome production under HG conditions (Fig. 3B). The present study also demonstrated that SOX9 downregulation inhibited HG-induced secretion of the pro-inflammatory cytokine IL-1β (Fig. 3C). These results demonstrated that the HG-induced inflammatory process was inhibited by SOX9 silencing in Müller cells.

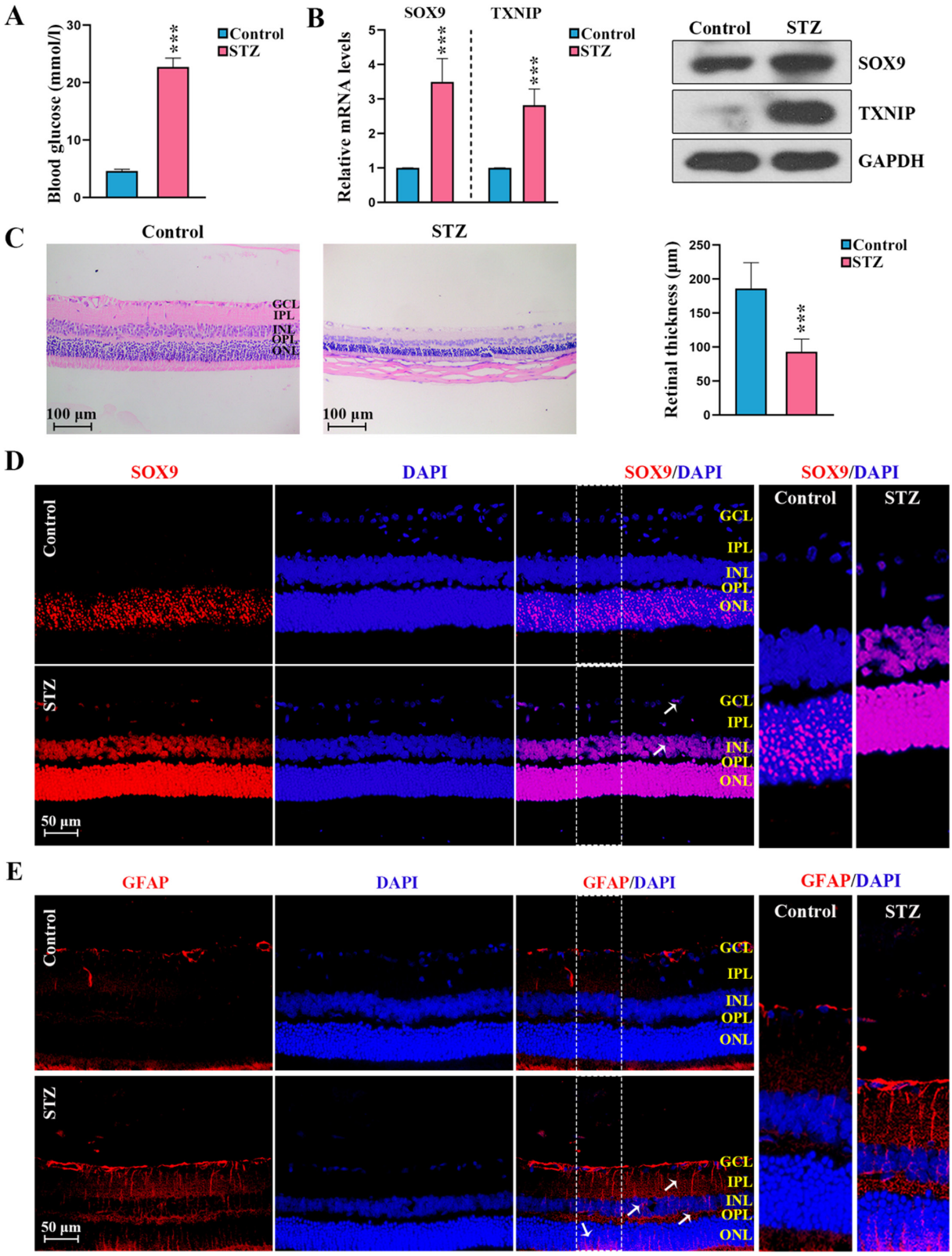

Fig. 1. SRY-box transcription factor 9 (SOX9) and thioredoxin-interacting protein (TXNIP) expression in the retina of streptozotocin (STZ)-induced diabetic rats. (A) Glucometric assessment of the blood glucose level in retina tissues. (B) The mRNA and protein levels of SOX9 and TXNIP were measured in retina tissues by real-time PCR and western blot. (C) Representative images of hematoxylin and eosin (H&E)-stained retinal sections from the control and STZ groups and quantification of the total retinal thickness. (D and E) Immunofluorescence staining for the expression of SOX9 and glial fibrillary acidic protein (GFAP) in the diabetic rat retina. Nuclei were fluorescently labeled with DAPI. SOX9, SRY-box transcription factor 9; TXNIP, thioredoxin-interacting protein; GCL, ganglion cell layer; IPL, inner plexiform layer; INL, inner nuclear layer; OPL, outer plexiform layer; ONL, outer nuclear layer. ***P<0.001 versus the control group.

 doi: 10.1538/expanim.22-0126

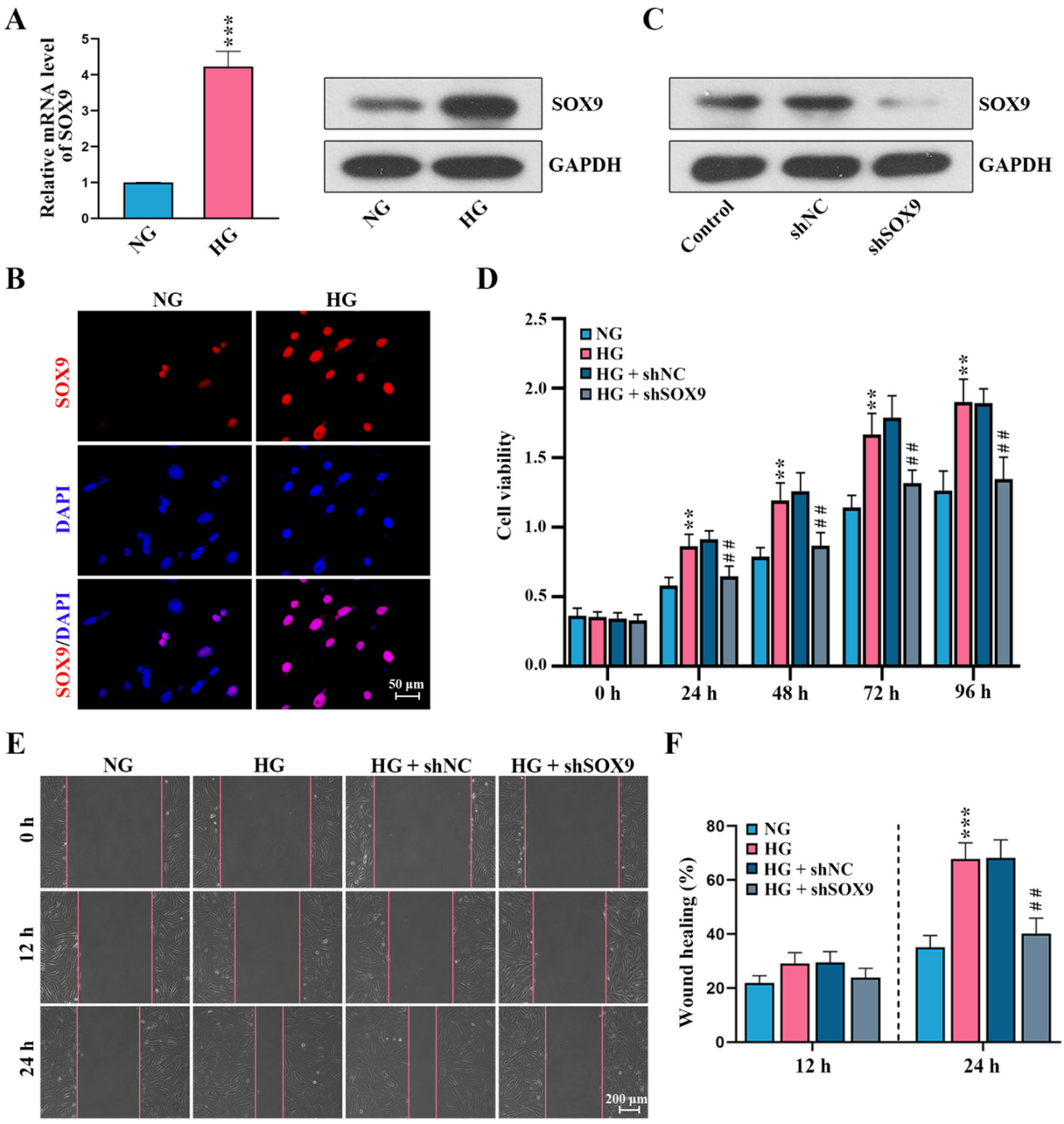

Fig. 2. Effect of SRY-box transcription factor 9 (SOX9) on cell proliferation and migration in HG-induced Müller cells. Müller cells were cultured in 5.5 mmol/l glucose (NG group) and 25 mmol/l glucose (HG group), respectively. (A) The expression of SOX9 after glucose treatments was detected by real-time PCR and western blot. (B) Immunofluorescence staining for the expression of SOX9 in the NG and HG groups. Müller cells were infected with a silenced SOX9 lentivirus or negative control. (C) Western blot was used to verify the efficiency of Müller cells at 72 h after lentivirus infection. The infected cells were subsequently treated with HG and the cells were used for the following assays. (D) An methyl thiazole tetrazolium (MTT) assay was conducted to assess cell viability at different points in time. (E) Representative images of the scratched areas at different time points are shown. (F) The rate of wound healing was assessed at 12 h and 24 h. NG, normal glucose; HG, high glucose. ***P<0.001 versus the NG group. $^{\#\#}P$<0.01 versus the HG + negative control shRNA (shNC) group.

SOX9 activates TXNIP by binding to the TXNIP promoter

TXNIP is considered a positive regulator of Müller cells gliosis, so we explored the relationship between TXNIP and SOX9. The present study indicated that the mRNA and protein levels of TXNIP in the HG group were higher than those in the control group and that SOX9 knockdown inhibited TXNIP expression in HG-treated Müller cells (Figs. 4A), indicating that SOX9 positively regulated TXNIP expression. Furthermore, a dual-luciferase assay was conducted to confirm the correlation between SOX9 and TXNIP. As indicated in Fig. 4B, SOX9 expression markedly upregulated the luciferase activity by targeting the *TXNIP* promoter, indicating

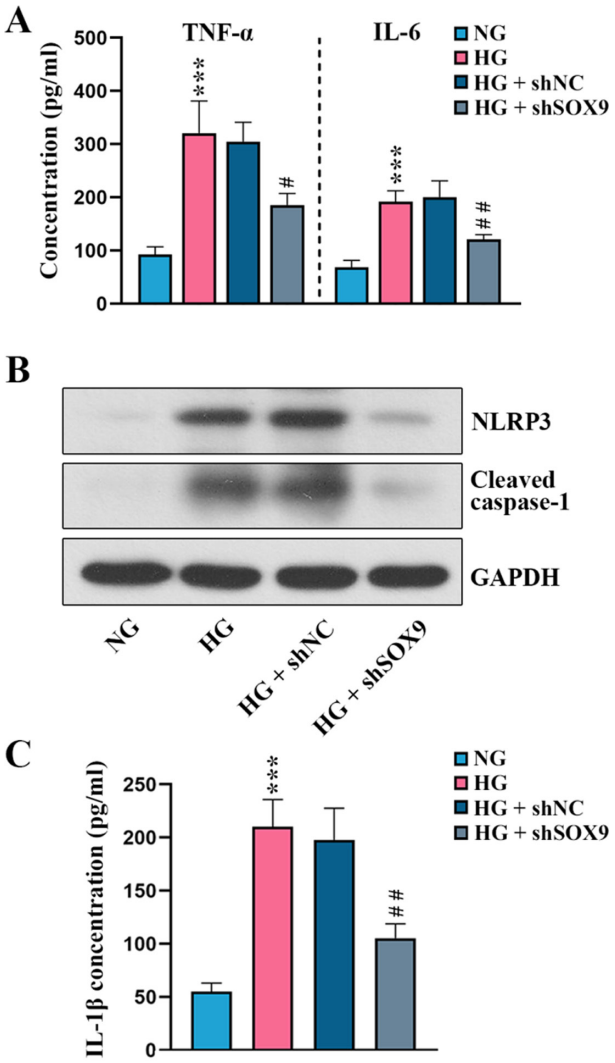

Fig. 3. Effect of SRY-box transcription factor 9 (SOX9) on inflammation in high glucose (HG)-induced Müller cells. After treatment with HG for 48 h, Müller cells were used for the following experiments. (A) The levels of tumor necrosis factor-α (TNF-α) and IL-6 were measured by ELISA. (B) Western blot analysis for the expression of NLRP3 and cleaved caspase-1. (C) The IL-1β level was measured by ELISA. ***P<0.001 versus the normal glucose (NG) group. #P<0.05 and ##P<0.01 versus the HG + negative control shRNA (shNC) group.

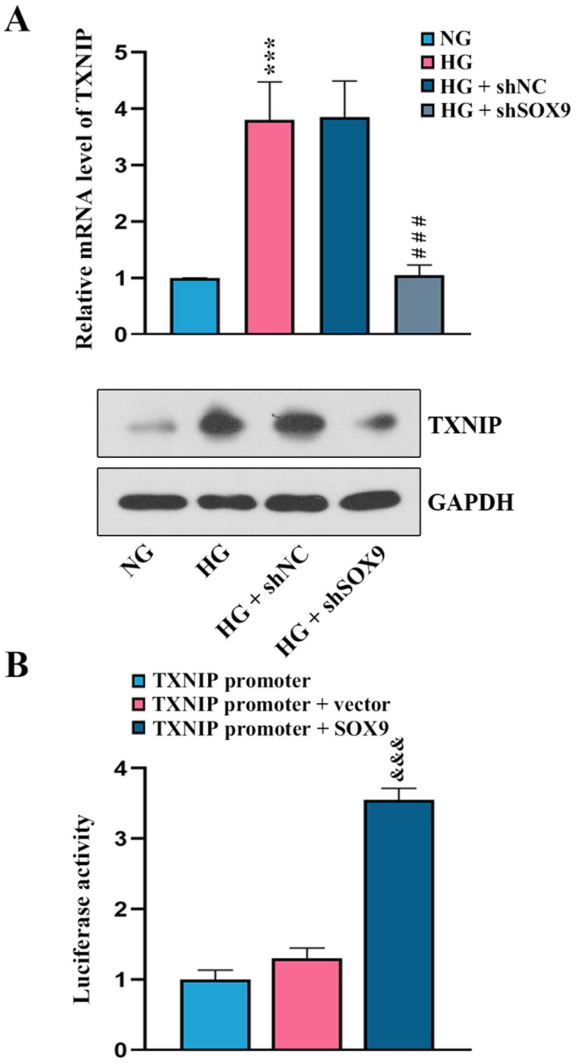

Fig. 4. Interaction between SRY-box transcription factor 9 (SOX9) and thioredoxin-interacting protein (TXNIP) in Müller cells. (A) The expression of TXNIP was detected in different groups by real-time PCR and western blot. (B) SOX9 overexpression and empty vectors were transfected into Müller cells with a vector containing the TXNIP promoter sequence, and the luciferase activity was determined at 48 h after transfection. ***P<0.001 versus the normal glucose (NG) group. ###P<0.001 versus the high glucose (HG) + negative control shRNA (shNC) group. &&&P<0.001 versus the TXNIP promoter + vector group.

that SOX9 could directly bind to the promoter of TXNIP and transcriptionally regulate TXNIP expression in Müller cells.

TXNIP overexpression reverses the cell functions of SOX9 in HG-induced Müller cells

Given that SOX9 activated TXNIP expression through binding to the TXNIP promoter, we further investigate whether TXNIP mediated the effect of SOX9 on Müller cell function. A lentivirus expressing TXNIP and empty vectors was constructed in SOX9-silenced Müller cells and treated with HG. As shown in Fig. 5A, the results showed that TXNIP expression was significantly reduced after SOX9 knockdown and that TXNIP overexpression increased the downregulated TXNIP level. Cell viability and wound healing assay results revealed that TXNIP overexpression reversed the repressive effects of SOX9 knockdown on Müller cell viability and migration (Figs. 5B and C). SOX9 knockdown decreased the release of IL-1β, and NLRP3 protein expression and TXNIP overexpression restored these changes (Figs. 5D and E). These findings suggested that SOX9 might exert its function in Müller cells by transcriptionally regulating TXNIP.

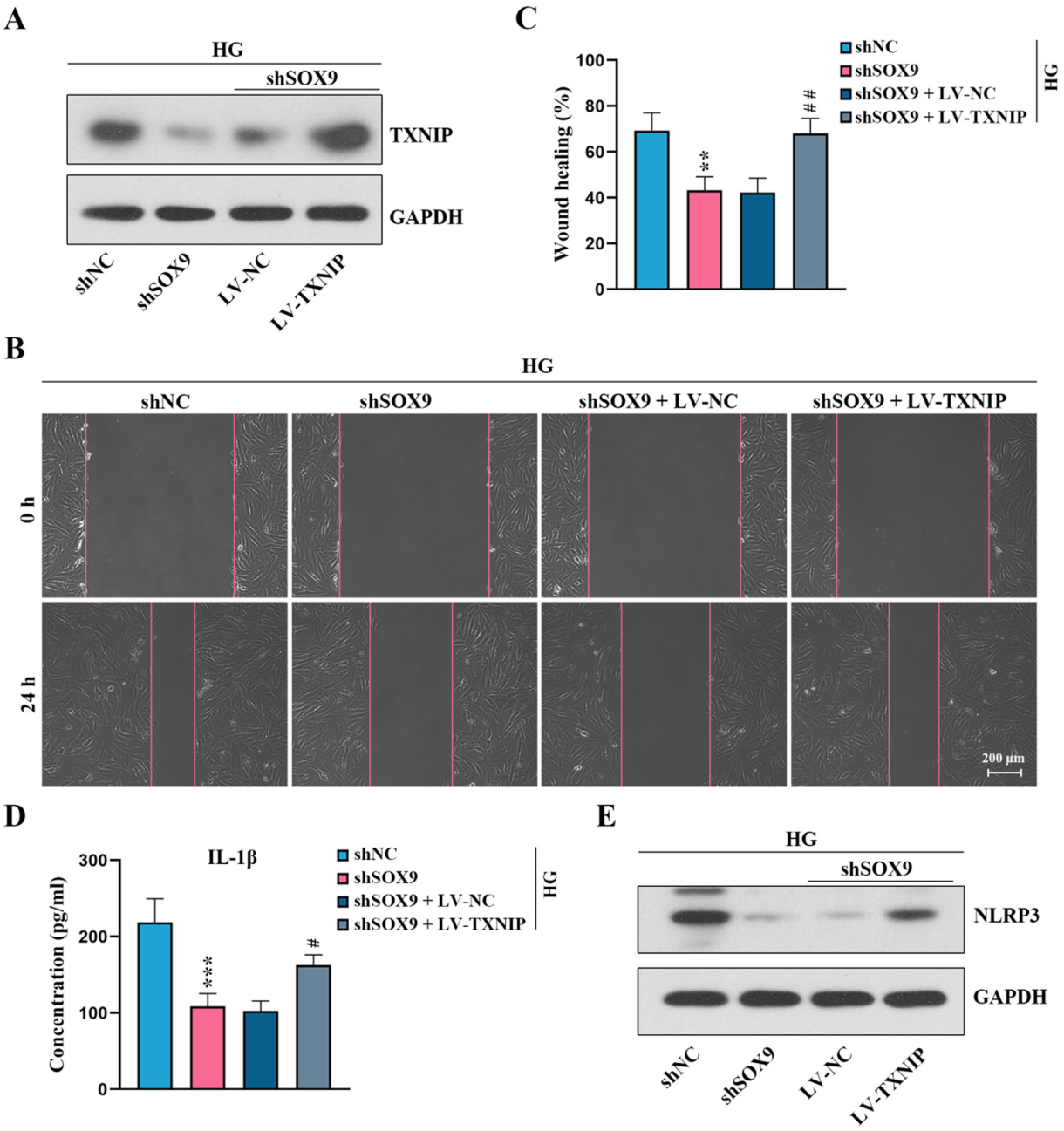

Fig. 5. Effect of thioredoxin-interacting protein (TXNIP) overexpression on SRY-box transcription factor 9 (SOX9)-mediated cell function in HG-stimulated Müller cells. The Müller cells co-infected with lentiviruses constructed for SOX9 knockdown and TXNIP overexpression and treated with high glucose (HG). (A) Western blot analysis for TXNIP after treatment with HG. (B) Representative images of the scratched areas at different time points. (C) The rate of wound healing was assessed at 24 h. (D) The IL-1β level was measured by ELISA at 48 h. (E) Western blot analysis for NLRP3 in Müller cells after treatment with HG for 48 h. $^{**}P<0.01$ and $^{***}P<0.001$ versus the HG + negative control shRNA (shNC) group. $^{\#}P<0.05$ and $^{\#\#}P<0.01$ versus the HG + shSOX9 + LV-NC group.

Discussion

DR is a common complication of diabetes and is the leading cause of vision loss [24]. Studies have demonstrated that further consequences, including the rupture of the blood-retinal barrier, retinal edema, and vision loss, occurred during the period of DR [25, 26]. However, the progression of DR is not yet treated or prevented effectively, leading to the rate of vision loss remaining surprisingly high [27, 28]. Therefore, in-depth study of the molecular mechanisms of DR is valuable and of clinical significance. In the present study, a DR rat model was successfully established by treating rats with STZ and the expression of SOX9 in retina was detected *in vivo*. The regulatory function of SOX9 in relation to HG-treated Müller cell function was further in-

vestigated *in vitro*. To explore the specific mechanism, the association between SOX9 and TXNIP was further explored by a dual-luciferase analysis. The results revealed that SOX9 was positively associated with TXNIP expression. Notably, TXNIP overexpression counteracted the repressive effects of SOX9 silencing under HG conditions. Collectively, data from the diabetes model proved that the regulation of SOX9 resulted in cell proliferation, cell migration, and inflammation by promoting TXNIP transcription, further aggravating the pathological processes of DR.

Commonly used STZ-induced rodent models show a rapid onset of type 1 diabetes and several symptoms of DR. Loss of retinal pericytes and capillaries, thickening of the vascular basement membrane, and increased vascular permeability have been reported in STZ-induced rats [29, 30]. In the present study, we found that the retinas tended to be thinner in STZ rats than in control rats, which was consistent with previous studies [23, 31]. In our study, a model of DR rats was successfully established, as evidenced by the elevation of the blood glucose concentration and decreased retina thickness. We also evaluated the role of SOX9 in STZ-treated rats with DR for the first time, and the results revealed that SOX9 and TXNIP expression was significantly increased both in DR rat retinas and HG-treated human retinal Müller cells. Previous studies reported that hyperglycemia caused an increase in SOX9 in pancreatic β-cells [32], and an increased level of SOX9 expression was observed in Müller cells of rats with light-induced retinal damage [33]. These cells were termed non-astrocytic inner retinal glial (NIRG) cells. It has also been demonstrated that cells expressing SOX9 were similar to Müller glia and retinal progenitors that cells that expressed SOX9 was found similar to Müller glia and retinal progenitors that were primarily scattered across the inner retinal layer [34]. In the present study, SOX9 was mainly expressed in the ONL in control rats, and there were no cells that were labeled for SOX9 in the INL or GCL. After STZ treatment, SOX9 expression extended into the INL and GCL in the diabetic retina, suggesting that increased SOX9 might promote the downstream activation of the pathways of inflammatory responses [35]. It has been well documented that hyperglycemia can increase the expression of GFAP in Müller cells [36, 37]. GFAP is recognized as an important marker of reactive gliosis in Müller cells after retinal injury [38]. It has also been reported that Müller cells are activated by elevated expression of GFAP in the early stages of DR [39]. In the present study, GFAP was restricted to the retinal nerve fiber layer in the control group. However, its immunoreactivity was augmented and extended into the inner and outer plexiform layers in the diabetic retina, which was consistent with a previous report [40], suggesting that STZ treatment partially caused gliosis.

Müller cells, the predominant retinal glial cells, are responsible for maintaining the structure of the blood-retinal barrier and ensuring the proper functioning of retinal neurons [41]. Recent evidence demonstrates that Müller cells are important drivers of DR [42]. More specifically, Müller cells have been shown to contribute to retinal damage by migrating to the vitreoretinal surface and releasing inflammatory cytokines [43, 44]. In this sense, physiological dysfunction of Müller cells may contribute to the progression of DR. Therefore, exploring the mechanisms and development of Müller cells in DR processes is crucial to establish an effective intervention and ultimately avoid vision impairment. It has been demonstrated that high glucose concentrations induced Müller cell dedifferentiation and favored their migration ability [9]. The present study demonstrated that HG treatment significantly promoted Müller cell proliferation and migration, and SOX9 knockdown decreased abnormal proliferation and migration of cells under hyperglycemia conditions. In addition, research on the progression of DR found that inflammatory cytokines, including IL-1β, TNF-α, IL-8, and IL-6 were highly expressed in diabetic rats [45, 46]. Consistently, results of the present study indicated that SOX9 knockdown decreased HG-induced inflammatory cytokines expression. Retinal inflammasome activation is an important factor for cell damage in DR. Li *et al.* found that the expression of NLRP3, cleaved caspase-1, and other inflammatory factors was upregulated in rat retinas of STZ-induced diabetic rats [47]. In our study, increased levels of inflammatory factors (NLRP3 and cleaved caspase-1) were regulated by SOX9 in Müller cells under HG conditions. Furthermore, the inflammatory reaction induces dysfunction of Müller cells, destroying the blood-retinal barrier and aggravating retinal dysfunction in persons with diabetes [48].

It has been demonstrated that the proliferation and migration of Müller cells increase capillary permeability and angiogenesis, further aggravating the severity of DR [49]. Given that SOX9 induced gliosis of Müller cells, which was accompanied by multiple biological reactions, including cell proliferation and migration, further discussion of the underlying mechanisms of DR is warranted. It is worth noting that vascular endothelial growth factor (VEGF) plays a definitive role in the disease, and VEGF has been found to drive the proliferation and migration of vascular cells and promote vascular permeability and angiogenesis [50]. It has also been reported that SOX9 is positively correlated with the ex-

pression of VEGF involved in active angiogenesis, and knockdown of SOX9 inhibited the expression of VEGF [51]. However, the association between SOX9 and VEGF expression was not investigated in the present study, and this may be an important area for future research.

It was shown recently that TXNIP exerts a key role in glucose metabolism. Ao *et al.* reported that TXNIP induced the proliferation of retinal cells under HG conditions [52]. Our study found that TXNIP was involved in the development of DR *in vivo* and *in vitro*. More importantly, a previous study reported that TXNIP knockdown inhibited cell migration and decreased VEGF-triggered retinal angiogenesis in DR [53]. These findings suggest that TXNIP exerts an important role in DR that involves in VEGF-related vascular angiogenesis. Previous studies confirmed that TXNIP transcription is regulated by multiple factors in the progression of DR. For instance, it was confirmed that TXNIP transcription is upregulated by carbohydrate response element-binding protein (Chrebp) in diabetic fatty (ZDF) rats [54]. It has also been reported that upregulation of SOX9 activated the transcription of Neurogenin-3, aggravating the severity of diabetes [55]. In our study, bioinformatics prediction revealed that SOX9 could target the region of the *TXNIP* promoter, further promoting TXNIP transcription. These results suggested that inhibition of SOX9 and TXNIP is an important target for the treatment of DR. In summary, the increased expression of SOX9 promoted the proliferation, migration, and inflammation by regulating TXNIP transcription.

Taken together, our data unraveled that SOX9 positively regulated gliosis in HG-treated Müller cells by targeting the *TXNIP* promoter. Meanwhile, glial cell proliferation, metastasis, and inflammation aggravated retinal dysfunction in persons with diabetes, further worsening the severity of DR. However, SOX9 knockdown inhibited these biological processes caused by HG. Conversely, TXNIP overexpression restored the effects caused by SOX9 silencing. These findings help elucidate a new regulatory mechanism of DR and provide a reference for clinical medicine.

Conflicts of Interest

The authors declared no conflict of interest.

Acknowledgments

This work was supported by the Science and Technology Planning Project of Liaoning Province (Natural Science Foundation of Liaoning Province; Grant No. 2021-MS-376).

References

1. Wang W, Lo ACY. Diabetic retinopathy: pathophysiology and treatments. Int J Mol Sci. 2018; 19: 1816. [Medline] [CrossRef]
2. Wilkinson CP, Ferris FL 3rd, Klein RE, Lee PP, Agardh CD, Davis M, et al. Global Diabetic Retinopathy Project Group. Proposed international clinical diabetic retinopathy and diabetic macular edema disease severity scales. Ophthalmology. 2003; 110: 1677–1682. [Medline] [CrossRef]
3. Li J, Li X, Lei M, Li W, Chen W, Ma T, et al. A prediction model for worsening diabetic retinopathy after panretinal photocoagulation. Diabetol Metab Syndr. 2022; 14: 124. [Medline] [CrossRef]
4. Leasher JL, Bourne RR, Flaxman SR, Jonas JB, Keeffe J, Naidoo K, et al. Vision Loss Expert Group of the Global Burden of Disease Study. Global estimates on the number of people blind or visually impaired by diabetic retinopathy: a meta-analysis from 1990 to 2010. Diabetes Care. 2016; 39: 1643–1649. [Medline] [CrossRef]
5. Liu C, Dong W, Lv Z, Kong L, Ren X. Thioredoxin-interacting protein in diabetic retinal neurodegeneration: A novel potential therapeutic target for diabetic retinopathy. Front Neurosci. 2022; 16: 957667. [Medline] [CrossRef]
6. Parmar UM, Jalgaonkar MP, Kulkarni YA, Oza MJ. Autophagy-nutrient sensing pathways in diabetic complications. Pharmacol Res. 2022; 184: 106408. [Medline] [CrossRef]
7. Portillo JC, Yu JS, Vos S, Bapputty R, Lopez Corcino Y, Hubal A, et al. Disruption of retinal inflammation and the development of diabetic retinopathy in mice by a CD40-derived peptide or mutation of CD40 in Müller cells. Diabetologia. 2022; 65: 2157–2171. [Medline] [CrossRef]
8. Symon A, Harley V. SOX9: A genomic view of tissue specific expression and action. Int J Biochem Cell Biol. 2017; 87: 18–22. [Medline] [CrossRef]
9. Sanhueza Salas LF, García-Venzor A, Beltramone N, Capurro C, Toiber D, Silberman DM. Metabolic imbalance effect on retinal müller glial cells reprogramming capacity: Involvement of histone deacetylase SIRT6. Front Genet. 2021; 12: 769723. [Medline] [CrossRef]
10. Wang X, Shu Q, Ni Y, Xu G. CRISPR-mediated SOX9 knockout inhibits GFAP expression in retinal glial (Müller) cells. Neuroreport. 2018; 29: 1504–1508. [Medline] [CrossRef]
11. Gajjala PR, Kasam RK, Soundararajan D, Sinner D, Huang SK, Jegga AG, et al. Dysregulated overexpression of Sox9 induces fibroblast activation in pulmonary fibrosis. JCI Insight. 2021; 6: 152503. [Medline] [CrossRef]
12. Zhang W, Cheng P, Hu W, Yin W, Guo F, Chen A, et al. Inhibition of microRNA-384-5p alleviates osteoarthritis through its effects on inhibiting apoptosis of cartilage cells via the NF-κB signaling pathway by targeting SOX9. Cancer Gene Ther. 2018; 25: 326–338. [Medline] [CrossRef]
13. Singh LP. Thioredoxin Interacting Protein (TXNIP) and pathogenesis of diabetic retinopathy. J Clin Exp Ophthalmol. 2013; 4: 10.4172/2155-9570.1000287. [Medline] [CrossRef]
14. Shalev A. Minireview: Thioredoxin-interacting protein: regulation and function in the pancreatic β-cell. Mol Endocrinol. 2014; 28: 1211–1220. [Medline] [CrossRef]
15. Chen W, Zhao M, Zhao S, Lu Q, Ni L, Zou C, et al. Activation of the TXNIP/NLRP3 inflammasome pathway contributes to inflammation in diabetic retinopathy: a novel inhibitory effect of minocycline. Inflamm Res. 2017; 66: 157–166. [Medline] [CrossRef]
16. Perrone L, Devi TS, Hosoya KI, Terasaki T, Singh LP. Inhibition of TXNIP expression in vivo blocks early pathologies of diabetic retinopathy. Cell Death Dis. 2010; 1: e65. [Medline] [CrossRef]
17. Sbai O, Devi TS, Melone MA, Feron F, Khrestchatisky M, Singh LP, et al. RAGE-TXNIP axis is required for S100B-

promoted Schwann cell migration, fibronectin expression and cytokine secretion. J Cell Sci. 2010; 123: 4332–4339. [Medline] [CrossRef]
18. Fan K, Ruan X, Wang L, Lu W, Shi Q, Xu Y. Circ_0004872 promotes platelet-derived growth factor-BB-induced proliferation, migration and dedifferentiation in HA-VSMCs via miR-513a-5p/TXNIP axis. Vascul Pharmacol. 2021; 140: 106842. [Medline] [CrossRef]
19. Devi TS, Lee I, Hüttemann M, Kumar A, Nantwi KD, Singh LP. TXNIP links innate host defense mechanisms to oxidative stress and inflammation in retinal Muller glia under chronic hyperglycemia: implications for diabetic retinopathy. Exp Diabetes Res. 2012; 2012: 438238. [Medline] [CrossRef]
20. Devi TS, Somayajulu M, Kowluru RA, Singh LP. TXNIP regulates mitophagy in retinal Müller cells under high-glucose conditions: implications for diabetic retinopathy. Cell Death Dis. 2017; 8: e2777. [Medline] [CrossRef]
21. Lalit PS, Thangal Y, Fayi Y, Takhellambam SD. Potentials of gene therapy for diabetic retinopathy: The use of nucleic acid constructs containing a TXNIP promoter. Open Access J Ophthalmol. 2018; 3: 147. [Medline]
22. Lupo G, Motta C, Giurdanella G, Anfuso CD, Alberghina M, Drago F, et al. Role of phospholipases A2 in diabetic retinopathy: in vitro and in vivo studies. Biochem Pharmacol. 2013; 86: 1603–1613. [Medline] [CrossRef]
23. Sadikan MZ, Nasir NAA, Iezhitsa I, Agarwal R. Antioxidant and anti-apoptotic effects of tocotrienol-rich fraction against streptozotocin-induced diabetic retinopathy in rats. Biomed Pharmacother. 2022; 153: 113533. [Medline] [CrossRef]
24. Pan HZ, Zhang H, Chang D, Li H, Sui H. The change of oxidative stress products in diabetes mellitus and diabetic retinopathy. Br J Ophthalmol. 2008; 92: 548–551. [Medline] [CrossRef]
25. Barber AJ, Gardner TW, Abcouwer SF. The significance of vascular and neural apoptosis to the pathology of diabetic retinopathy. Invest Ophthalmol Vis Sci. 2011; 52: 1156–1163. [Medline] [CrossRef]
26. Hu WK, Liu R, Pei H, Li B. Endoplasmic reticulum stress-related factors protect against diabetic retinopathy. Exp Diabetes Res. 2012; 2012: 507986. [Medline] [CrossRef]
27. Yu X, Xu Z, Mi M, Xu H, Zhu J, Wei N, et al. Dietary taurine supplementation ameliorates diabetic retinopathy via anti-excitotoxicity of glutamate in streptozotocin-induced Sprague-Dawley rats. Neurochem Res. 2008; 33: 500–507. [Medline] [CrossRef]
28. Kowluru RA, Chan PS. Oxidative stress and diabetic retinopathy. Exp Diabetes Res. 2007; 2007: 43603. [Medline] [CrossRef]
29. Cai X, McGinnis JF. Diabetic retinopathy: animal models, therapies, and perspectives. J Diabetes Res. 2016; 2016: 3789217. [Medline] [CrossRef]
30. Grossniklaus HE, Kang SJ, Berglin L. Animal models of choroidal and retinal neovascularization. Prog Retin Eye Res. 2010; 29: 500–519. [Medline] [CrossRef]
31. Sheskey SR, Antonetti DA, Rentería RC, Lin CM. Correlation of retinal structure and visual function assessments in mouse diabetes models. Invest Ophthalmol Vis Sci. 2021; 62: 20. [Medline] [CrossRef]
32. Zhang YN, Fu DX, Xu JX, Wang GY. The effect of SOX9 on islet β cells in high glucose environment through regulation of ERK/P38 signaling pathway. Eur Rev Med Pharmacol Sci. 2019; 23: 8476–8484. [Medline]
33. Wang X, Fan J, Zhang M, Ni Y, Xu G. Upregulation of SOX9 in Glial (Müller) cells in retinal light damage of rats. Neurosci Lett. 2013; 556: 140–145. [Medline] [CrossRef]
34. Ning K, Sendayen BE, Kowal TJ, Wang B, Jones BW, Hu Y, et al. Primary cilia in amacrine cells in retinal development. Invest Ophthalmol Vis Sci. 2021; 62: 15. [Medline] [CrossRef]
35. Bautista-Pérez R, Cano-Martínez A, Gutiérrez-Velázquez E, Martínez-Rosas M, Pérez-Gutiérrez RM, Jiménez-Gómez F, et al. Spinach methanolic extract attenuates the retinal degeneration in diabetic rats. Antioxidants. 2021; 10: 717. [Medline] [CrossRef]
36. Oosuka S, Kida T, Oku H, Horie T, Morishita S, Fukumoto M, et al. Effects of an aquaporin 4 inhibitor, TGN-020, on murine diabetic retina. Int J Mol Sci. 2020; 21: 2324. [Medline] [CrossRef]
37. Rungger-Brändle E, Dosso AA, Leuenberger PM. Glial reactivity, an early feature of diabetic retinopathy. Invest Ophthalmol Vis Sci. 2000; 41: 1971–1980. [Medline]
38. Guidry C. The role of Müller cells in fibrocontractive retinal disorders. Prog Retin Eye Res. 2005; 24: 75–86. [Medline] [CrossRef]
39. Qiu AW, Liu QH, Wang JL. Blocking IL-17A Alleviates diabetic retinopathy in rodents. Cell Physiol Biochem. 2017; 41: 960–972. [Medline] [CrossRef]
40. Zhu M, Gao S, Gao S, Wang Y, Li N, Shen X. Interleukin-17A attenuates photoreceptor cell apoptosis in streptozotocin-induced diabetic mouse model. Bioengineered. 2022; 13: 14175–14187. [Medline] [CrossRef]
41. Coughlin BA, Feenstra DJ, Mohr S. Müller cells and diabetic retinopathy. Vision Res. 2017; 139: 93–100. [Medline] [CrossRef]
42. Ghaseminejad F, Kaplan L, Pfaller AM, Hauck SM, Grosche A. The role of Müller cell glucocorticoid signaling in diabetic retinopathy. Graefes Arch Clin Exp Ophthalmol. 2020; 258: 221–230. [Medline] [CrossRef]
43. Portillo JC, Lopez Corcino Y, Miao Y, Tang J, Sheibani N, Kern TS, et al. CD40 in retinal Müller cells induces P2X7-dependent cytokine expression in macrophages/microglia in diabetic mice and development of early experimental diabetic retinopathy. Diabetes. 2017; 66: 483–493. [Medline] [CrossRef]
44. Suzumura A, Kaneko H, Funahashi Y, Takayama K, Nagaya M, Ito S, et al. n-3 Fatty Acid and its metabolite 18-HEPE ameliorate retinal neuronal cell dysfunction by enhancing Müller BDNF in diabetic retinopathy. Diabetes. 2020; 69: 724–735. [Medline] [CrossRef]
45. Zhong Y, Li J, Chen Y, Wang JJ, Ratan R, Zhang SX. Activation of endoplasmic reticulum stress by hyperglycemia is essential for Müller cell-derived inflammatory cytokine production in diabetes. Diabetes. 2012; 61: 492–504. [Medline] [CrossRef]
46. Giblin MJ, Smith TE, Winkler G, Pendergrass HA, Kim MJ, Capozzi ME, et al. Nuclear factor of activated T-cells (NFAT) regulation of IL-1β-induced retinal vascular inflammation. Biochim Biophys Acta Mol Basis Dis. 2021; 1867: 166238. [Medline] [CrossRef]
47. Li S, Yang H, Chen X. Protective effects of sulforaphane on diabetic retinopathy: activation of the Nrf2 pathway and inhibition of NLRP3 inflammasome formation. Exp Anim. 2019; 68: 221–231. [Medline] [CrossRef]
48. Tang L, Zhang C, Lu L, Tian H, Liu K, Luo D, et al. Melatonin maintains inner blood-retinal barrier by regulating microglia inhibition of PI3K/Akt/Stat3/NF-κB signaling pathways in experimental diabetic retinopathy. Front Immunol. 2022; 13: 831660. [Medline] [CrossRef]
49. Ma C, Shi ZH, Han XY, Liu C, Yan B, Du JL. Targeting circRNA-MAP4K2 for the treatment of diabetes-induced retinal vascular dysfunction. Aging (Albany NY). 2022; 14: 6255–6268. [Medline] [CrossRef]
50. Simó R, Sundstrom JM, Antonetti DA. Ocular Anti-VEGF therapy for diabetic retinopathy: the role of VEGF in the pathogenesis of diabetic retinopathy. Diabetes Care. 2014; 37: 893–899. [Medline] [CrossRef]
51. Goto S, Onishi A, Misaki K, Yonemura S, Sugita S, Ito H, et al. Neural retina-specific Aldh1a1 controls dorsal choroidal vascular development via Sox9 expression in retinal pigment epithelial cells. eLife. 2018; 7: e32358. [Medline] [CrossRef]
52. Ao H, Li H, Zhao X, Liu B, Lu L. TXNIP positively regulates

the autophagy and apoptosis in the rat müller cell of diabetic retinopathy. Life Sci. 2021; 267: 118988. [Medline] [CrossRef]
53. Yan J, Deng J, Cheng F, Zhang T, Deng Y, Cai Y, et al. Thioredoxin-interacting protein inhibited vascular endothelial cell-induced HREC angiogenesis treatment of diabetic retinopathy. Appl Biochem Biotechnol. 2023; 195:1268–1283. [Medline]
54. Chen K, Lang H, Wang L, Liu K, Zhou Y, Mi M. *S-Equol* ameliorates insulin secretion failure through Chrebp/Txnip signaling via modulating PKA/PP2A activities. Nutr Metab (Lond). 2020; 17: 7. [Medline] [CrossRef]
55. Lynn FC, Smith SB, Wilson ME, Yang KY, Nekrep N, German MS. Sox9 coordinates a transcriptional network in pancreatic progenitor cells. Proc Natl Acad Sci USA. 2007; 104: 10500–10505. [Medline] [CrossRef]